

# A Compact Band-Notched UWB MIMO Antenna with Enhanced Isolation Using Comb Shaped Decoupling Element

Soumya CHATTERJEE<sup>1</sup>, Sekhar RANA<sup>2</sup>, Rajarshi SANYAL<sup>2</sup>

<sup>1</sup>Dept. of Electronics & Communication Engineering, Pailan College of Management & Technology, Kolkata, W.B, India

<sup>2</sup>Dept. of Electronics & Communication Engineering, MCKV Institute of Engineering, Howrah, W.B, India

soumya.8021@gmail.com, sekhar.rana1983@gmail.com, rajarshi.sanyal1972@gmail.com

Submitted May 17, 2022 / Accepted December 5, 2022 / Online first March 6, 2023

**Abstract.** A compact 37 mm × 26 mm two element multiple-input-multiple-output (MIMO) antenna is presented for ultra wide band (UWB) system application with band notched characteristics. The proposed antenna comprises of two semi trapezoidal shaped monopole radiating the enhanced isolation, comb shaped symmetrical stub arrangement are embedded at the U shaped etched elements. The band rejection feature around 3.5 GHz has been achieved by incorporating the open ended quarter wavelength spiral shaped slot resonator on the patched surface. In order to realize periphery to the stepped ground plane between the monopole radiators. This novel design approach leads towards isolation enhancement better than 20 dB throughout the UWB spectral range (3.1–10.6 GHz) with peak isolation near about 46 dB. The Envelope Correlation Coefficient is significantly lower than 0.005 in the entire operating range except the WiMAX rejection band.

## Keywords

Ultra-wide band (UWB), MIMO, isolation, Envelope Correlation Coefficient (ECC)

## 1. Introduction

The ultra-wide band is modern technology that offers a large band width (3.1–10.6 GHz). Ultra-wide band (UWB) multiple-input-multiple-output (MIMO) antenna has gained its potential among the researchers due to its high data rate and improved transmission quality without the need of extra bandwidth or power. Hence it is able to mitigate multi-path fading problem [1]. The MIMO antenna comprises at least two monopole radiating elements at moderate separation. Some of the literatures also recorded for the 5G MIMO antenna with eight numbers of antenna elements [2]. In order to suppress the mutual coupling effects, various decoupling embedding techniques have been adopted in previous literatures. The previous investigation predominantly emphasized on the stub incorporation

techniques, such as Inverted F-shaped stub pair [3], slot edged T-shaped stub [4], Inverted L-shaped stub pair [5], [6], T-shaped protrude metallic stub [7], novel G-shaped stub [8] or the radial stub loaded resonators [9] that are effective decoupling structures to diminish the dominance of mutual coupling between the planar monopole radiators. In another discussion the substrate integrated waveguide based approach has been proposed in recent work for terahertz range application [10]. Metamaterial unit cell series type parasitic element incorporation between the monopole radiating elements is a good approach to achieve the better isolation [11]. Based on the principle of microstrip multimode resonator, decoupling structure has been configured which connects the partial ground plane of MIMO UWB antenna in [12]. Neutralization line decoupling structure provides very high isolation as discussed in [13]. Orthogonal placement of the antenna elements also leads towards the high isolation in absence of decoupling circuit [14]. Multilayered electronic band gap structure is also the effective decoupling structure in order to realize the potential mutual coupling reduction [15]. Carbon black film coating as a conductor back plane plays a crucial role regarding the mutual coupling reduction [16]. Mutual coupling reduction using fence-type decoupling structure also been proposed in [17]. Parasitic reflectors can produce the additional coupling path and creates a reverse current to cancel out the mutual coupling between the monopole radiators, so that the improved isolation more than 25 dB can be attained as recorded in [18]. In recent investigation vertical stub along with centrally truncated H-shaped slot has been employed to realize the isolation improvement up to 18 dB [19]. Early investigation also reveals mutual coupling mitigation by using antenna interference cancellation chip which occupies the compact volume which is responsible for the improvement of passive isolation [20]. UWB isolation has been maintained ( $|S_{21}| \leq -17$  dB) by using metallic via connection strategy which is another modified approach for mutual effect suppression as discussed in [21].

This paper mainly intended to design the half trapezoidal shaped two elements band notched UWB-MIMO antenna. The mutual coupling reduction strategy of this

proposed antenna has been influenced from the early works where tree shaped ground plane stub incorporation has been revealed [22] where the increased number of tree branches contributes for the additional resonance and weakens the mutual coupling. The isolation improvement is significantly high in higher frequency band however isolation suffers a bit particularly for the lower UWB operating range. This aforesaid strategy has been modified in this paper where the train of narrow grid shaped stub inclusion with equal and closer separation inside the U shaped slotted decoupling structure has the remarkable wide stop band characteristics with multiple resonances. Hence the notable mutual coupling suppression ( $|S_{21}| \leq -20$  dB &  $ECC \leq 0.005$ ) over the entire UWB spectral range of 3.1–11 GHz can be achieved. The excellence of the comb shaped decoupling stub integrated within the U-shaped etched periphery in the ground plane particularly focuses on its simplified geometry as compared to the tree like structure. The introduction of the parallel narrow metallic quarter wavelength stub grid contributes for the multiple additional current paths which ultimately decouple the energy from antennas and parallel current path shares the induced mutual current. Therefore significant blocking of the coupled current to the other port can be achieved. Another fascinating feature of this work is the band rejection capability in UWB spectral span. Different band notched resonators have been discussed in earlier works such as inverted  $\pi$  shaped slotted resonator [23], electromagnetic band gap with split ring resonator [24], T shaped stepped impedance resonator [25], parasitic micro-strip resonator [26]. The spiral shaped quarter wavelength slotted open ended resonator has the effective contribution regarding the band rejection characteristics. The band rejection characteristics around 3.5 GHz to evade the narrow band WiMAX inference has been successfully accomplished with the help of  $\lambda_g/4$  open ended spiral shaped slotted resonator.

## 2. Semi Trapezoidal Band-Notch UWB-MIMO Antenna

### 2.1 Introduction

The novel band notched MIMO-UWB antenna structure composed of two semi trapezoidal shaped monopole radiating elements with structural simplicity with exaggerate performance especially for the mutual coupling suppression viewpoint is designed. Proper impedance matching between the ground plane and monopole radiator exhibits the usable operating bandwidth from 3 GHz to 11 GHz. Open ended  $\lambda_g/4$  long meandered slot resonator (where  $\lambda_g$  is the guided wavelength at 3.5 GHz) is mounted in both the radiator surface as a filter element. Comb shaped stub type decoupling element in conjunction with U shaped truncation plays an important role to mitigate the correlation effect between two nearby radiators. The pro-

posed decoupling concept resulted for effective isolation ( $|S_{21}| \leq -20$  dB) over the entire UWB range. Isolation depth has been improved noticeably over 40 dB in several small segments of the UWB spectrum especially for the higher operating frequency.

### 2.2 Configuration of Trapezoidal Shaped Two-Element Band-Notched MIMO-UWB Antenna

The conventional monopole radiator design is fundamentally a compact structure which provides UWB operation with WiMAX band notch function. The two symmetrical semi trapezoidal radiating monopoles are mounted side by side with neighboring vertical edge as illustrated in Fig. 1. The maximum length to width ratio is approximately 5.14 which allows the long current path and better realization regarding lower frequency cut-off edge could be accepted. The gap between the radiator and the upper periphery of the ground plane is so adjusted that could maintained the higher frequency impedance matching in UWB range. FR-4 material with  $\epsilon_r = 4.4$  and thickness of 1.6 mm is used as the antenna substrate. The integrated filter network with the monopole radiators is an open ended quarter wavelength meandered slot structure corresponding to the targeted rejection resonance of 3.5 GHz. The meandered resonator is responsible for strong perturbation and the monopole elements are unable to radiate around the desired stop band. The effective length  $L_n$  of the resonator is empirically approximated as

$$L_n = \frac{c}{4f_n \sqrt{\epsilon_{r\text{eff}}}} \quad (1)$$

where  $c$  is velocity of light in free space,  $f_n$  is notch resonance frequency and  $\epsilon_{r\text{eff}} = (\epsilon_r + 1) / 2$ ,  $\epsilon_r$  is the relative permittivity of the substrate and  $L_n = L_1 + L_2 + L_3 + L_4 + L_5 - 4t$ . The rear part of the antenna comprises truncated ground plane with comb shaped stub elements.

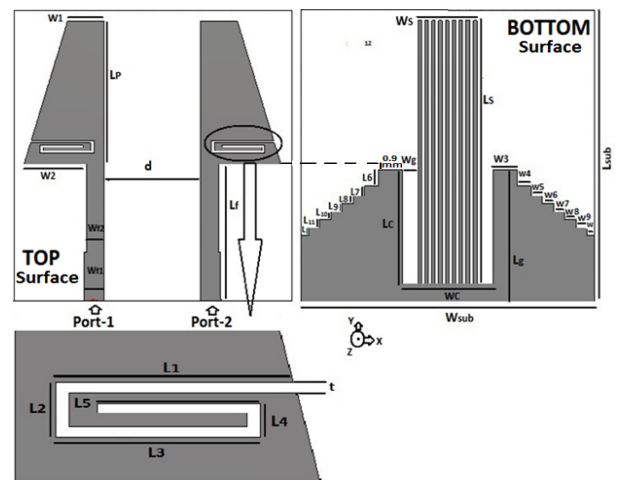


Fig. 1. Geometry of the proposed trapezoidal shaped band notched MIMO-UWB antenna.

### 2.3 Design Steps for Isolation Improvement

The mutual coupling suppression is an essential issue for the MIMO antenna where the separation between radiators always creates a mutual effect in a serious extent. In this work comb, shaped decoupling component has been introduced on the rear side of planar radiators along with U shaped metallic etching. Figure 2 presents successive structural development of decoupling circuit. Primarily the location of radiating elements are so placed that makes edge to edge spacing  $d = 0.14\lambda_1$  where  $\lambda_1$  is the lower cutoff wavelength of the operating band with respect to guided wave. Therefore the insertion loss ( $|S_{21}|$ ) depth exhibits almost negligible response because strong mutual coupling between the radiators becomes an influencing factor. For the normal two element band notched MIMO-UWB configuration (Antenna-1) without inserting any decoupling structure, excessive mutual coupling between two neighboring monopole radiators occurs. Further the incremental development is U shaped etched periphery at the mid portion of ground plane referred as Antenna-2 design; it contributes for the better isolation near rejection band. However the isolation performance for higher operating range is not up to the mark. The I-shaped stub addition orthogonal to the ground plane on the opposite side of the monopole radiator which has been originated from the center of the U shaped peripheral cut is referred as Antenna-3. This makes a dramatic change for the isolation characteristics throughout the UWB spectrum. The effective length of the I-shaped stub is  $\lambda_g/2$  corresponding to notch resonance of 3.5 GHz. The physical explanation of incremental decoupling can be affirmed as the stub mainly has an inductive behavior and the nonmetallic gap between the inner edge of U type truncation and the metallic stub introduces band stop resonances. This nature finally helps to decouple mid part or the upper part of the operating capacitive behavior which consequently leads to the multiple UWB band firmly.

The proposed comb shaped decoupling structure is referred as Antenna-4 where multiple narrow slits have been introduced inside the wide I shaped metallic stub. Narrow and close separation of multiple metallic strips of the comb shaped stub element stimulates the stop band resonances strongly that dips down the insertion loss extremely which deeply concerned with the rising isolation. The novelty of this proposed decoupling structure particularly lies in its parallel coupled narrow metallic stub geometry and the separation between the truncated edge of the ground plane and the stub elements. The reduction of the wide metallic stub width into the multiple symmetrical narrow metallic stub grids enhances the inductive effect of stub element remarkably and the closer metallic etched surface between successive narrow metallic grids introduces very high capacitive effect. Hence due to the inclusion of multiple parallel inductive and capacitive effects, a wide band stop filtration capability can be considered based on the introduction of multiple parallel LC resonators. The dimension of the gap between the edge of the stub and the ground plane also contributes to the additional capacitive effect. Therefore, the different capacitive effects lead to the different band stop filtration characteristics which eventually become responsible for the multiple resonances in the transmission coefficient.

### 2.4 Simulated Results

#### 2.4.1 Reflection Coefficient

The comparative reflection coefficient of all four antenna structures as shown in Fig. 2 are illustrated in Fig. 3. It has been assumed that port-1 is excited and port-2 is terminated from  $50 \Omega$  load and vice versa. The reflection coefficient of the proposed antenna (Antenna-4) exhibits excellent impedance matching UWB band with multiple pass band resonances except the narrow frequency range around 3.5 GHz which assures the WiMAX band rejection ability of the proposed antenna. Moreover the proposed antenna (Antenna-4) exhibits better impedance matching and eventually the reflection coefficient improves significantly for pass band.

#### 2.4.2 Tuning Characteristics of the Rejection Band

Figure 4 shows the tuning characteristics of the proposed antenna with varying open ended meandered slot length. When the length of meandered slot is reduced, the notched band shifted towards the higher frequency whereas the negligible effect can be observed in antenna performance.

#### 2.4.3 Isolation Characteristics

Mutual coupling effect between two monopole radiators of the band notched MIMO-UWB antenna are minimized by using the combination of U slot and stub combination. Figure 5 illustrates the comparative port isolation of all four antenna structures as mentioned in Fig. 2. As ob-

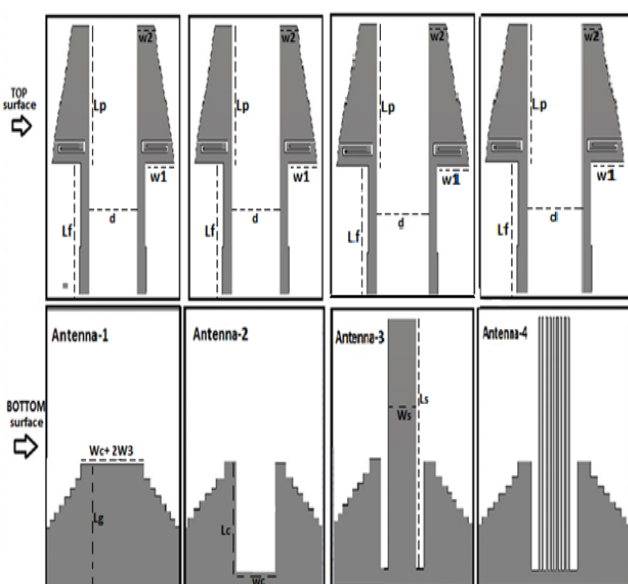


Fig. 2. Design steps of antenna to realize improved isolation characteristics.

served in figure that for Antenna-2, the U shaped etching process helps to improve the isolation especially at rejection frequency and throughout the UWB operating band. However at higher UWB frequency range additional resonant effect cannot be observed properly. The insertion of I shaped ground plane stub of Antenna-3 exhibits additional resonance effect which ultimately leads to the improved isolation achievement. Finally isolation characteristics for the proposed Antenna-4 structure exhibit the noticeable improvement of isolation especially at higher UWB range. Actually the comb shaped decoupling structure contributes to the decomposition of the original mutual coupling energy by producing multiple coupling paths which has been created by the large number of narrow metallic strip. This

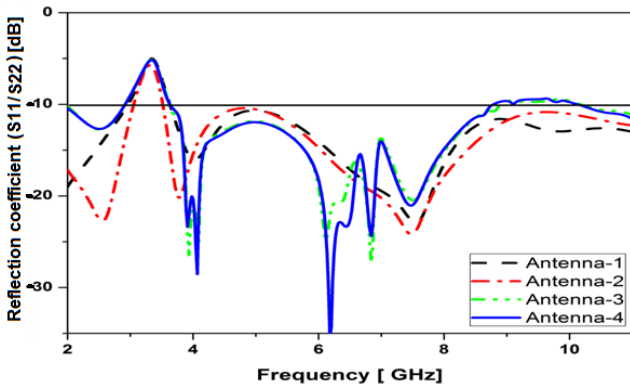


Fig. 3. Comparative reflection coefficient of Antenna-1 to Antenna-4 (proposed).

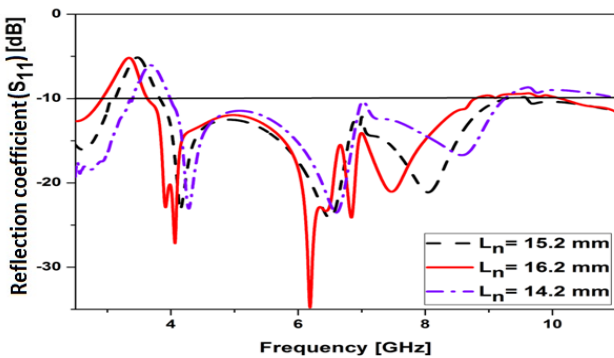


Fig. 4. Simulated reflection coefficient for varying length of meandered slot resonator.

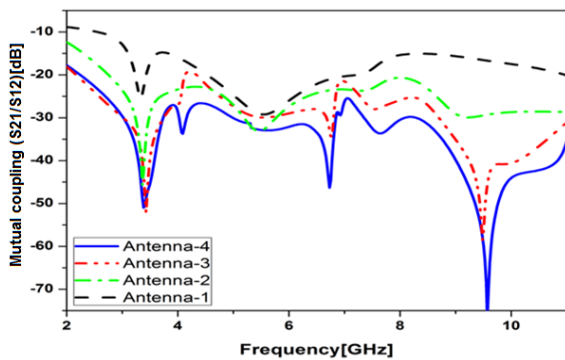


Fig. 5. Comparative isolation characteristics of Antenna-1 to Antenna-4 (proposed).

structure makes a significant reduction in mutual coupling of the other antenna element. The comb shaped novel ground plane stub extension from the U shaped truncated periphery of the ground plane is an effective and novel design approach which not only enhances the isolation ( $|S_{21}| \leq -20$  dB) in the entire UWB frequency range but also the peak isolation improvement at rejection band as well as higher UWB frequency band also been achieved. All the results of the proposed designs clearly indicate the suitability of the proposed band notched MIMO-UWB antennas in modern wireless system.

### 2.4.4 Surface Current Distribution

Figure 6 depicts the surface current distribution at 3.5 GHz where Port-1 is excited and Port-2 is matched by  $50 \Omega$  load. It is observed that the surface current mainly concentrated around the spiral shaped resonator. On the other hand, isolation improvement of the comb shaped decoupling elements has been justified by the surface current distribution analogy. Here the improved peak isolation leads towards the potential surface current concentration around the ground embedded decoupling excited Port-1. Furthermore the comprehension of the mutual coupling reduction mechanism and the significance of the narrow metallic etching of the incorporated stub can be assisted by the illustration and explanation of the surface current distribution at the peak isolation resonance at 9.5 GHz as depicted in Fig. 7. The surface current with conventional ground plane in Fig. 7(a) exhibits high mutual coupling among the radiators where Port-1 is excited and Port-2 is terminated with the  $50 \Omega$  matching load. The etched U-shaped decoupling structure on the ground plane reduces the mutual coupling effect. However, a good amount of current is still coupled with the other radiator. In the next development as shown in Fig. 7(b), the incorporation of ground plane I shaped stub inside the U-shaped truncated periphery reduces the mutual coupling efficiently by suppressing the ground current flowing between the radiating elements. In spite of this occurrence, a very less current still tends to couple with the other radiator and certain amount of ground current also exists due to the short ground strip adjacent to the other radiator as shown in the simulated Fig. 7(c) between two monopole radiators.

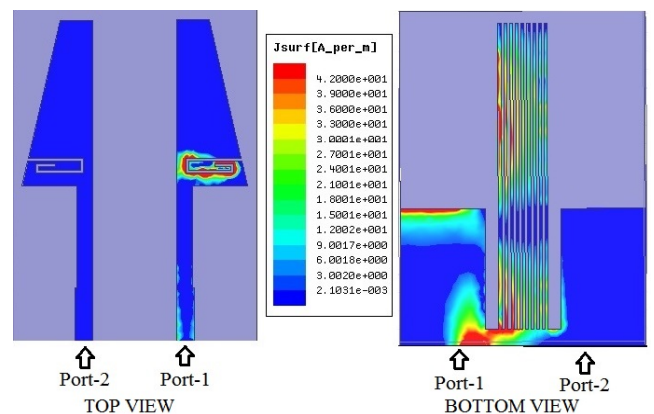


Fig. 6. Surface current distribution at 3.5 GHz (Port-1 excited).

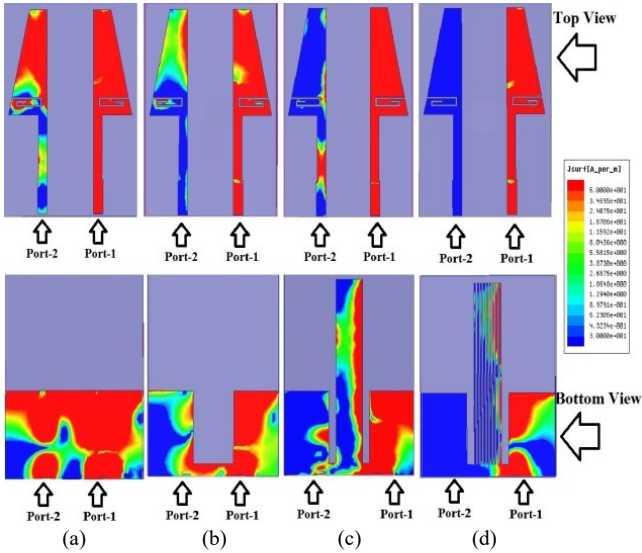


Fig. 7. Surface current distribution at 9.5 GHz (Port-1 excited).

The fascinating feature of the comb-shaped stub is the introduction of multiple parallel coupled conducting paths. The narrow metallic grid of the comb shaped stub at the proximity of the monopole radiator with excited port draws the maximum current. Therefore due to the strong coupling between the edge stub and the corresponding monopole radiator with excited port, a significant amount of surface current is induced to the narrow strip closer to the excited port. The intensity of the induced surface current gradually deteriorates for the successive metallic stub grid. Finally, the farthest metallic stub grid has almost negligible surface current concentration as shown in Fig. 7(d) which ultimately provides very high isolation.

### 2.5 Measured Results

To verify the proposed design of two element semi trapezoidal shaped band notched MIMO-UWB antenna, a prototype has been fabricated on FR-4 substrate as shown in Fig. 8. The optimized design parameters are tabulated in

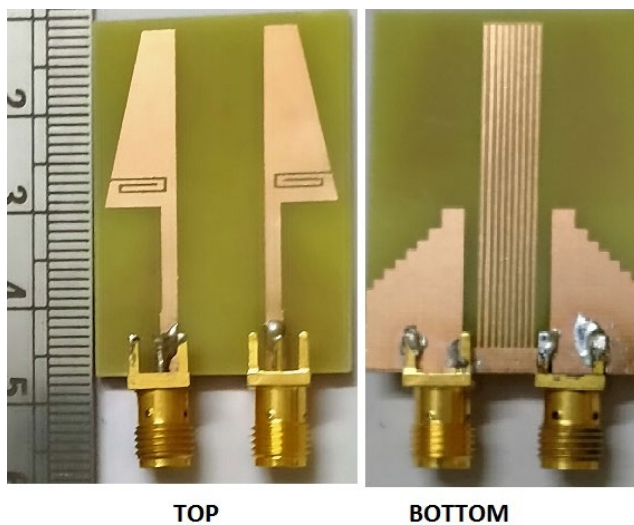


Fig. 8. Fabricated prototype of the proposed antenna.

Parameter	Dimension (mm)	Parameter	Dimension (mm)
$L_{sub}$	37	$W_s$	5.2
$W_{sub}$	26	$W_c$	8
$L_f$	17.4	$W_g$	1.4
$W_{f1}$	1.86	$L_1$	5.8
$W_{f2}$	1.66	$L_2$	1.6
$L_p$	18	$L_3$	5
$L_s$	33	$L_4$	1
$L_c$	13	$L_5$	4
$L_g$	16.6	$L_6$	2
$L_7$	1.2	$W_4$	1.2
$L_8$	1	$W_5$	1
$L_9$	1	$W_6$	1
$L_{10}$	1	$W_7$	1
$L_{11}$	1	$W_8$	1
$L$	1	$W_9$	1
$W_1$	3.5	$W$	0.6
$W_2$	6	$d$	9
$W_3$	2.2	$t$	0.3

Tab. 1. Optimized dimension of the parameters of Fig. 1.

Tab. 1 to ensure the band notch characteristics as well as the minimization of mutual coupling between two monopole radiators.

#### 2.5.1 Reflection Coefficient and Isolation

The experimental reflection coefficient ( $|S_{11}|$ ) and the isolation ( $|S_{21}|$ ) are plotted in Fig. 9 and Fig. 10 only for the excitation of Port-1 and load termination of Port-2. The measured impedance bandwidth of the proposed structure is from 3 GHz to 11 GHz for  $|S_{11}| \leq -10$  dB along with the rejection band covering frequency ranging from

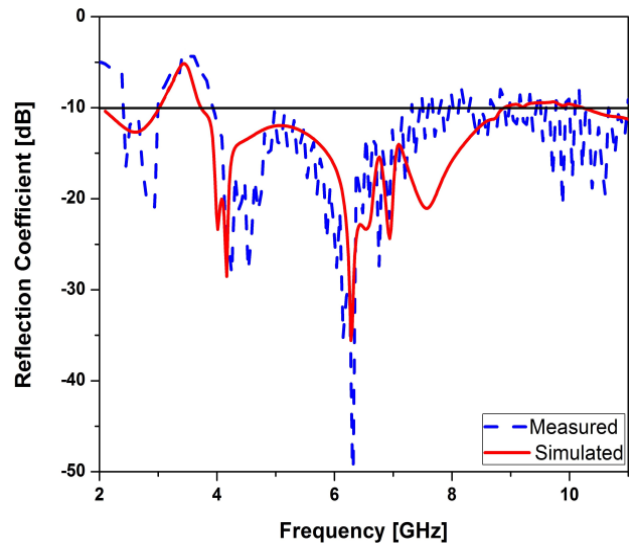


Fig. 9. Measured and simulated reflection coefficient ( $|S_{11}|$ ).

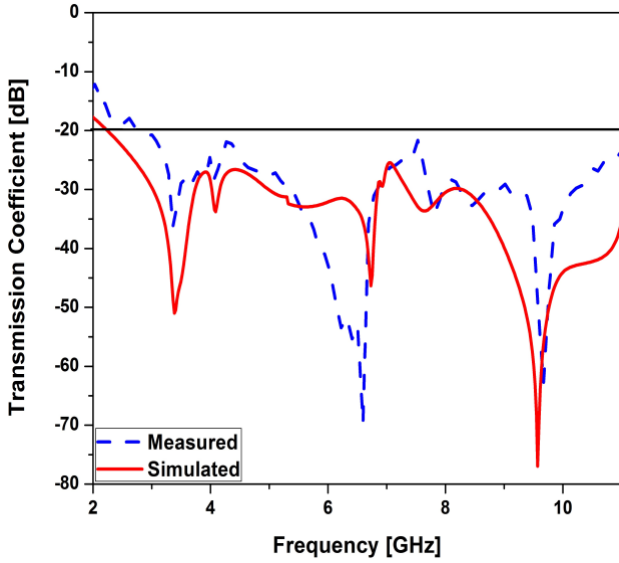


Fig. 10. Measured and simulated transmission coefficient ( $|S_{21}|$ ).

3.1 GHz to 3.6 GHz which can validate the band notch mechanism for WiMAX band. It can also be observed that measured port isolation ( $|S_{21}|$ ) is below  $-20$  dB throughout the UWB operating range along with the peak isolation below  $-48$  dB. Though the measured isolation near 6 GHz slightly become worse due to the tolerance of manufacturing and measurement environment. However multiple  $|S_{21}|$  notches in higher UWB range ultimately are indicating the acceptable consideration of the isolation characteristics for practical application.

### 2.5.2 Envelope Correlation Coefficient

Exploration of diversity for band notched UWB-MIMO antenna is a decisive factor which acquaint for isolation capability. Diversity performance is always characterized by envelope correlation coefficient (ECC) formulated as [9]

$$\rho = \frac{|S_{11}^* S_{12} + S_{21}^* S_{22}|^2}{(1 - |S_{11}|^2 - |S_{21}|^2)(1 - |S_{22}|^2 - |S_{12}|^2)} \quad (2)$$

where  $S_{11}$  and  $S_{22}$  are the reflection coefficient of radiator-1 and radiator-2 while the insertion loss represented by  $S_{12}$  or  $S_{21}$  corresponding to the mutual effect of radiator-1 on radiator-2.  $S_{11} = S_{22}$  and  $S_{12} = S_{21}$ . ECC of both the simulated and measured reflection loss characteristics and isolation has been shown in Fig. 11. Figure 11 shows the good parity between simulated and measured results. It has been found that Peak ECC at central notch frequency is less than 0.035 otherwise ECC of entire operating pass band notably less than 0.005 in entire UWB spectral range. Low value of ECC for the proposed structure implies for the negligible correlation performance.

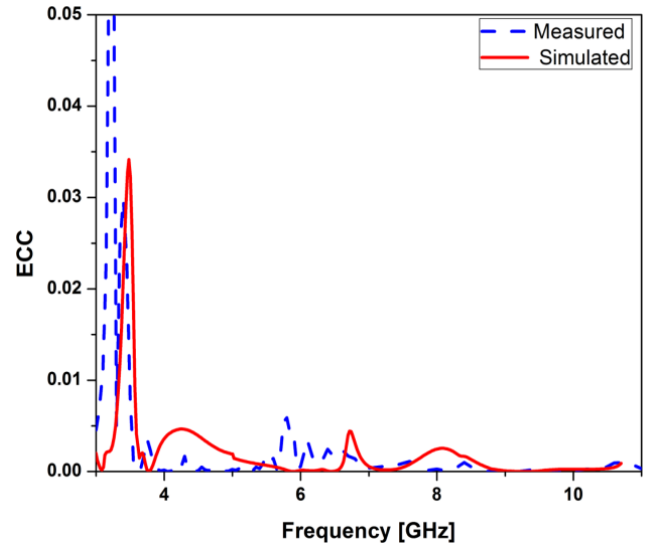


Fig. 11. Envelope correlation coefficient (ECC).

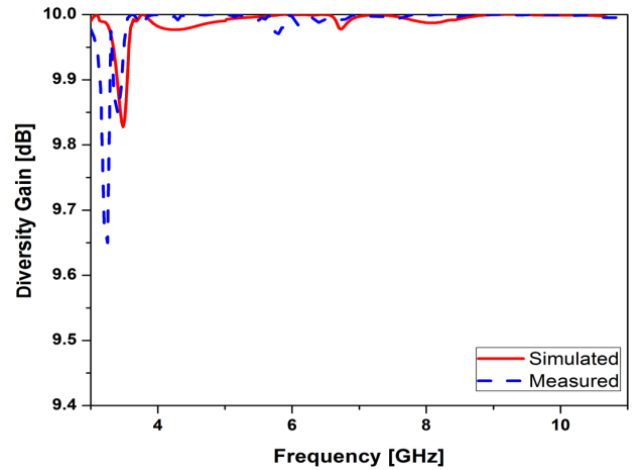


Fig. 12. Diversity gain of the proposed antenna.

### 2.5.3 Pattern Diversity Gain

Pattern diversity gain is strictly influenced by ECC in two antenna systems. The approximated formulation of diversity gain is given as [9]

$$PDG = 10 \times \sqrt{1 - |\rho|} \quad (3)$$

where 10 is the maximum value of the diversity gain. It is generally expressed in terms of dB unit. With sharp declining of ECC value, deterioration of pattern diversity gain becomes faster. Figure 12 shows the simulated and measured differential gain. As observed, near the rejection band around 3.5 GHz, diversity gain dips down sharply to 9.7 dB. However almost flat response near 10 dB can be observed for the whole UWB spectrum. Therefore higher PDG is a fair indicator to determine the uncorrelated operation of two element MIMO antennas.

2.5.4 Radiation Characteristics

Far-field radiation patterns for YZ-plane and XZ-plane have been plotted in Fig. 13(a), (b) where it has been considered that Port-1 is excited and Port-2 is terminated with 50 Ω matching load. The results illustrate that YZ-plane co-polarization pattern at 7 GHz is monopole-like dumb-bell shaped however at higher frequency of 10 GHz,

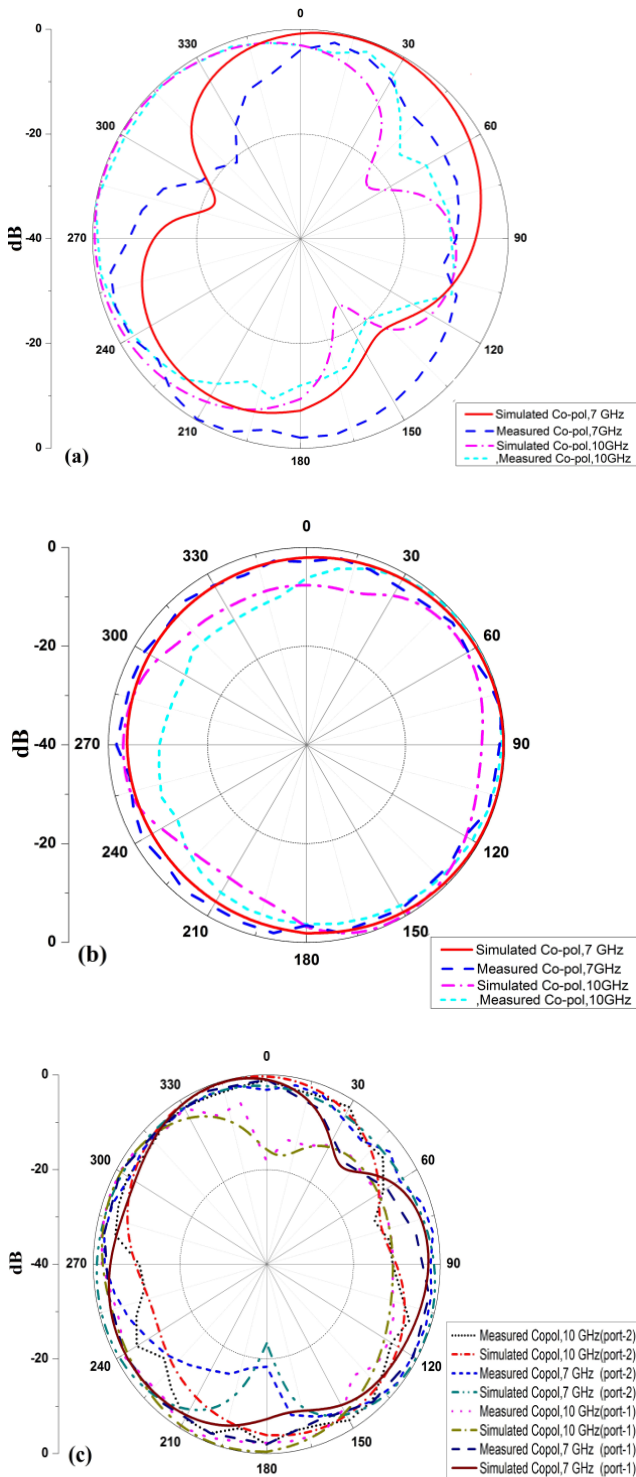


Fig. 13. Measured radiation patterns of the proposed antenna: (a) YZ-plane (Port-1 excited), (b) XZ-plane (Port-1 excited) and (c) XY-plane (Port-1 or Port-2 excited).

it can be observed that co-polarized pattern is not a complete dumb-bell shaped and does not have two sided null. On the other hand, XZ-plane patterns still have omnidirectional nature for both 7 and 10 GHz. However it can be seen that omni-directional characteristics deteriorates at higher frequency of 10 GHz due to excitation of higher order resonant mode. The radiation pattern diversity of the proposed MIMO UWB antenna has been justified by illustrating the XY-plane patterns as shown in Fig. 13(c). It can be observed that both simulated and measured radiation patterns at 7 GHz and 10 GHz tend to cover complementary space region. The radiation null at 7 GHz can be seen at the angle of 40 degrees from X axis with the excitation of Port-1 while the radiation pattern with Port-2 excitation at same frequency is almost at its maximum. Similarly at 10 GHz, the radiation null with Port-1 excitation can be observed at 180 degrees from X axis while radiation pattern with Port-2 excitation possesses a high value of -3.7 dB. The complementary pattern at 10 GHz has also been observed at the radiation null at 0 degree with Port-2 excitation while the pattern of excited Port-1 attains its maximum value of -1.5 dB. From above discussion, it can be concluded that null of the radiation pattern of one monopole radiator is always covered by the other monopole radiator which entails suitability of the proposed antenna for diversity system. The peak gain versus frequency of the proposed antenna has been illustrated in Fig. 14. Port-1 of the antenna is excited while Port-2 is terminated with 50 Ω load.

2.5.5 Peak Gain and Radiation Efficiency

As observed in Fig. 14 and Fig. 15 the simulated and measured results of the peak gain as well as radiation efficiency are in good agreement. The range of the measured peak gain varies from 0.9 dBi to 1.8 dBi for the entire UWB impedance bandwidth except the rejection band whose frequency range is from 3.4 GHz to 3.7 GHz. The sharp dip down of peak gain of -1.1 dBi at the central rejection band of 3.5 GHz can be seen. The variation of peak gain other than rejection band peak gain is about 0.9 dBi which is acceptable regarding the wider operational bandwidth of UWB-MIMO antenna. Similarly Figure 15 reveals that the radiation efficiency is above 85% throughout the operating range except the rejection band.

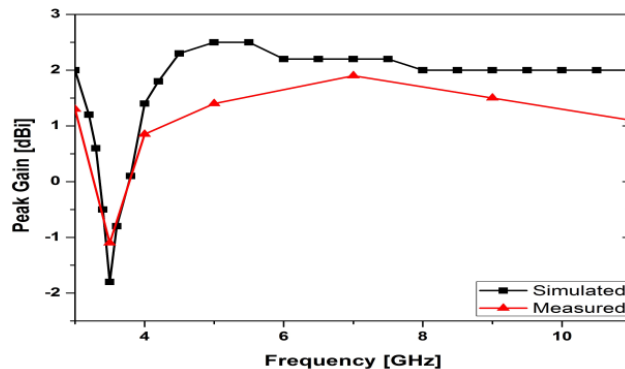


Fig. 14. Simulated and measured peak gain.

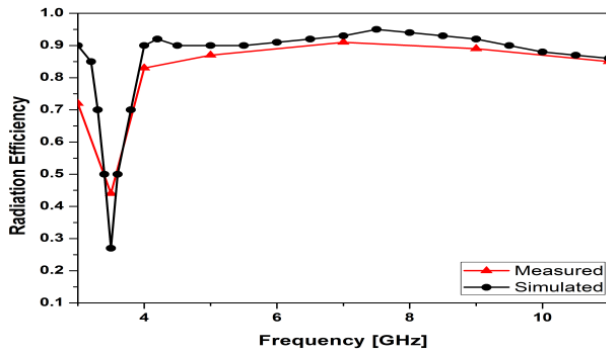


Fig. 15. Simulated and measured radiation efficiency.

### 3. Comparison with Previous Reported Designs

Table 2 summarizes the comparative studies of the proposed antenna with previous reported MIMO antennas. The table clearly shows the excellence of the proposed antenna in terms of isolation characteristics, ECC and compactness.

Ref.	Dimension [mm <sup>2</sup> ]	Isolation [dB]	ECC	Decoupling Element
[2]	140 × 70	> 11	< 0.08	Stepped impedance resonator
[6]	18 × 35	> 20	< 0.035	T-shape stubs
[7]	16 × 26	> 18	< 0.08	Stubs and protruded strips
[8]	18 × 36	> 20	< 0.05	Elliptical T-shaped stubs
[10]	85 × 85	> 25	NA	SIW
[9]	31.8 × 60	> 15	< 0.03	Radial stub loaded resonator
[17]	50 × 35	> 25	< 0.04	Fence type
[18]	16 × 28	> 20	< 0.04	Parasitic reflectors
[19]	18 × 35	> 18	< 0.0005	Vertical stub and H-slot
[21]	40 × 40	> 17	< 0.03	N/A
[22]	40 × 35	> 20	NA	Tree shaped stub
[15]	75 × 75	> 30	NA	Periodic multilayer EBG
[13]	79 × 55	> 30	NA	Neutralization line
Proposed Antenna	37 × 26	> 20	< 0.005	Comb shaped stub and U-slot

Tab. 2. Comparison of the proposed antenna with recently reported works.

### 4. Conclusion

Two-element planar band notched UWB antenna for MIMO application has been proposed in this article. The design configuration comprises semi-trapezoidal shaped monopole radiating elements. In order to mitigate the interference of WiMAX (3.3 GHz to 3.7 GHz) band in UWB spectral range, spiral shaped resonator has been incorporated with the monopole radiating pair. The installation of multiple patches inevitably causes mutual coupling between the nearby monopole radiators. Therefore a novel comb shaped decoupling stub element inside the truncated periphery of the ground plane has been embedded on the rear side of the MIMO antenna elements. This design approach significantly suppress the mutual coupling ( $S_{21} \leq -20$  dB) over the entire UWB spectral range (3.1 to 10.6 GHz). Excellent diversity performance with very low ECC ( $< 0.005$ ) accesses the suitability of the proposed band notched MIMO-UWB antennas in modern wireless system.

### Acknowledgments

The author would like to acknowledge Dr. Partha Pratim Sarkar, Dept. of Engg. & Technological Studies, University of Kalyani, India for the measurements.

### References

- [1] UL HAQ, M. A., KOZIEL, S. Ground plane alterations for design of high-isolation compact wideband MIMO antenna. *IEEE Access*, 2018, vol. 6, p. 48978–48983. DOI: 10.1109/ACCESS.2018.2867836
- [2] LI, J., ZHANG, X., WANG, Z., et al. Dual-band eight-antenna array design for MIMO applications in 5G mobile terminals. *IEEE Access*, 2019, vol. 7, p. 71636–71644. DOI: 10.1109/ACCESS.2019.2908969
- [3] IQBAL, A., SARAEREH, O. A., AHMAD, A. W., et al. Mutual coupling reduction using F-shaped stubs in UWB-MIMO antenna. *IEEE Access*, 2018, vol. 6, p. 2755–2759. DOI: 10.1109/ACCESS.2017.2785232
- [4] LI, W., HEI, Y., GRUBB, P. M., et al. Compact inkjet-printed flexible MIMO antenna for UWB applications. *IEEE Access*, 2018, vol. 6, p. 50290–50298. DOI: 10.1109/ACCESS.2018.2868707
- [5] CHANDEL, R., GAUTAM, A. K., RAMBABU, K. Tapered fed compact UWB MIMO-diversity antenna with dual band-notched characteristics. *IEEE Transactions on Antennas and Propagation*, 2018, vol. 66, no. 4, p. 1677–1684. DOI: 10.1109/TAP.2018.2803134
- [6] BAHMANZADEH, F., MOHAJERI, F. Simulation and fabrication of a high-isolation very compact MIMO antenna for ultra-wide band applications with dual band-notched characteristics. *AEU - International Journal of Electronics and Communications*, 2020, vol. 128, p. 1–8. DOI: 10.1016/j.aue.2020.153505

- [7] ADDEPALLI, T., ANITHA, V. R. A very compact and closely spaced circular shaped UWB MIMO antenna with improved isolation. *AEU-International Journal of Electronics and Communications*, 2020, vol. 114, p. 1–13. DOI: 10.1016/j.aeue.2020.153016
- [8] KHAN, M. I., KHATTAK, M. I. Designing and analyzing a modern MIMO-UWB antenna with a novel stub for stop band characteristics and reduced mutual coupling. *Microwave and Optical Technology Letters*, 2020, vol. 62, no. 10, p. 3209–3214. DOI: 10.1002/mop.32425
- [9] LI, Y., LI, W., YU, W. A multi-band/UWB MIMO/diversity antenna with an enhanced isolation using radial stub loaded resonator. *ACES Journal*, 2013, vol. 28, no. 1, p. 8–20.
- [10] ALIBAKHSHI-KENARI, M., VIRDEE, B. S., LIMITI, E. Study on isolation and radiation behaviors of a 34×34 array-antennas based on SIW and meta surface properties for applications in terahertz band over 125–300 GHz. *Optik - International Journal for Light and Electron Optics*, 2019, vol. 206, p. 1–10. DOI: 10.1016/j.ijleo.2019.163222
- [11] IQBAL, A., SARAEREH, O. A., BOUAZIZI, A., et al. Meta material based highly isolated MIMO antenna for portable wireless communication. *Electronics*, 2018, vol. 7, no. 10, p. 1–8. DOI: 10.3390/electronics7100267
- [12] ALI, W. A. E., IBRAHIM, A. A. A compact double-sided MIMO antenna with an improved isolation for UWB applications. *AEU-International Journal of Electronics and Communications*, 2017, vol. 82, p. 7–13. DOI: 10.1016/j.aeue.2017.07.031
- [13] LUO, S., LI, Y., XIA, Y., et al. A low mutual coupling antenna array with gain enhancement using meta material loading and neutralization line structure. *ACES Journal*, 2019, vol. 34, no. 3, p. 411–418.
- [14] SIPAL, D., ABEGAONKAR, M. P., KOUL, S. K. Easily extendable compact planar UWB MIMO antenna array. *IEEE Antennas and Wireless Propagation Letters*, 2017 vol. 16, p. 2328–2331. DOI: 10.1109/LAWP.2017.2717496
- [15] JIANG, T., JIAO, T., LI, Y. A low mutual coupling MIMO antenna using periodic Multi-Layered Electromagnetic Band Gap Structures. *ACES Journal*, 2018, vol. 33, no. 3, p. 305–311.
- [16] LIN, G. S., SUNG, C. H., CHEN, J. L., et al. Isolation improvement in UWB MIMO antenna system using carbon black Film. *IEEE Antennas and Wireless Propagation Letters*, 2017, vol. 16, p. 222–225. DOI: 10.1109/LAWP.2016.2570301
- [17] WANG, L., DU, Z., YANG, H., et al. Compact UWB MIMO antenna with high isolation using fence-type decoupling structure. *IEEE Antennas and Wireless Propagation Letter*, 2019, vol. 18, no. 8, p. 1641–1645. DOI: 10.1109/LAWP.2019.2925857
- [18] ADDEPALLI, T., ANITHA, V. R. Compact two-port MIMO antenna with high isolation using parasitic reflectors for UWB, X and Ku band applications. *Progress In Electromagnetics Research C*, 2020, vol. 102, p. 63–77. DOI: 10.2528/PIERC20030402
- [19] MASOODI, I., ISHTEYAQ, I., MUZAFFAR, K., et al. A compact band-notched antenna with high isolation for UWB MIMO applications. *International Journal of Microwave and Wireless Technologies*, 2021, vol. 13, p. 634–640. DOI: 10.1017/S1759078720001427
- [20] ZHAO, L., LIU, F., SHEN, X., et al. A high-pass antenna interference cancellation chip for mutual coupling reduction of antennas in contiguous frequency bands. *IEEE Access*, 2018, vol. 6, p. 38097–38105. DOI: 10.1109/ACCESS.2018.2853709
- [21] SAAD, A. A. R., MOHAMED, H. A. A conceptual design of a compact four element UWB MIMO slot antenna array. *IET Microwave, Antennas and Propagation*, 2019, vol. 13, no. 2, p. 208–215. DOI: 10.1049/iet-map.2018.5163
- [22] ZHANG, S., YING, Z., XIONG, J., et al. Ultra wideband MIMO/diversity antennas with a tree-like structure to enhance wideband isolation. *IEEE Antennas and Wireless Propagation Letters*, 2009, vol. 8, p. 1279–1282. DOI: 10.1109/LAWP.2009.2037027
- [23] LI, Y., LI, W., YE, Q. A reconfigurable triple-notch-band antenna integrated with defected micro strip structure band-stop filter for ultra-wideband cognitive radio applications. *International Journal of Antennas and Propagation*, 2013, vol. 13, p. 1–13. DOI: 10.1155/2013/472645
- [24] ABBAS, A., HUSSAIN, N., LEE, J., et al. Triple rectangular notch UWB antenna using EBG and SRR. *IEEE Access*, 2020, vol. 9, p. 2508–2515. DOI: 10.1109/ACCESS.2020.3047401
- [25] LI, Y., LI, W., YE, Q. A compact circular slot UWB antenna with multimode reconfigurable band-notched characteristics using resonator and switch techniques. *Microwave and Optical Technology Letters*, 2014, vol. 56, no. 3, p. 570–574. DOI: 10.1002/mop.28152
- [26] ARSHED, T., TAHIR, F. A. A miniaturized triple band-notched UWB antenna. *Microwave and Optical Technology Letters*, 2017, vol. 59, no. 10, p. 2581–2586. DOI: 10.1002/mop.30787

## About the Authors...

**Soumya CHATTERJEE** has obtained his AMIE degree in Electronics and Communication Engineering and M.Tech in Radio Physics from University of Calcutta. Currently he is associated as an Assistant Professor in Pailan College of Management & Technology Kolkata. His area of interest includes micro-strip antenna, micro-strip filter, frequency selective surfaces.

**Sekhar RANA** has obtained his B.Tech in Electronics and Communication Engineering from Jalpaiguri Govt. Engineering College and his M.Tech from Jadavpur University. His area of interest includes antenna and digital signal processing. Presently he is associated with MCKV Institute of Engineering as an Assistant Professor.

**Rajarshi SANYAL** has obtained his AMIETE and M.Tech. Degree in Electronics and Communication. He has obtained Ph.D. (Engg.) from the University of Kalyani. His area of research includes micro-strip antenna and Frequency Selective Surfaces. Presently he is associated with MCKV Institute of Engineering as an Assistant Professor.